

Accepted Manuscript

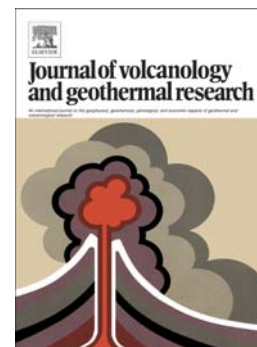
A contribution to the hazards assessment at Copahue volcano (Argentina-Chile) by facies analysis of a recent pyroclastic density current deposit

C. Balbis, I.A. Petrinovic, S. Guzmán

PII: S0377-0273(16)30252-9
DOI: doi: [10.1016/j.jvolgeores.2016.08.009](https://doi.org/10.1016/j.jvolgeores.2016.08.009)
Reference: VOLGEO 5908

To appear in: *Journal of Volcanology and Geothermal Research*

Received date: 26 January 2016
Revised date: 9 August 2016
Accepted date: 12 August 2016



Please cite this article as: Balbis, C., Petrinovic, I.A., Guzmán, S., A contribution to the hazards assessment at Copahue volcano (Argentina-Chile) by facies analysis of a recent pyroclastic density current deposit, *Journal of Volcanology and Geothermal Research* (2016), doi: [10.1016/j.jvolgeores.2016.08.009](https://doi.org/10.1016/j.jvolgeores.2016.08.009)

This is a PDF file of an unedited manuscript that has been accepted for publication. As a service to our customers we are providing this early version of the manuscript. The manuscript will undergo copyediting, typesetting, and review of the resulting proof before it is published in its final form. Please note that during the production process errors may be discovered which could affect the content, and all legal disclaimers that apply to the journal pertain.

**A contribution to the hazards assessment at Copahue volcano
(Argentina-Chile) by facies analysis of a recent pyroclastic density
current deposit**

Balbis, C. ^{a,*}, I.A. Petrinovic^a, S. Guzmán ^b

^a CICTERRA (CONICET-UNC). Av. Vélez Sarsfield 1611, Córdoba, Argentina. c.balbis@hotmail.com,

ipetrinovic@yahoo.com

^b Instituto de Bio y Geociencias del NOA (IBIGEO), UNSa-CONICET, 9 de Julio 14, 4405, Rosario de Lerma,

Salta, Argentina. sguzman@conicet.gov.ar

*Corresponding author

Abstract

We recognised and interpreted a recent pyroclastic density current (PDC) deposit at the Copahue volcano (Southern Andes), through a field survey and a sedimentological study. The relationships between the behaviour of the PDCs, the morphology of the Río Agrio valley and the eruptive dynamics were interpreted. We identified two lithofacies in the deposit that indicate variations in the eruptive dynamics: i) the opening of the conduit and the formation of a highly explosive eruption that formed a diluted PDC through the immediate collapse of the eruptive column; ii) a continued eruption which followed immediately and records the widening of the conduit, producing a dense PDC. The eruption occurred in 2000 AD, was phreatomagmatic ($VEI \leq 2$), with a vesiculation level above 4000 m depth and fragmentation driven by the interaction of magma with an hydrothermal system at ca. 1500 m depth. As deduced from the comparison between the accessory lithics of this deposit and those of the 2012 AD eruption, the depth of onset of vesiculation and fragmentation level in this volcano is constant in depth. In order to reproduce the distribution pattern of this PDC's deposit and to simulate potential PDC's forming-processes, we made several computational modelling from "denser" to "more diluted" conditions. The latter fairly reproduces the distribution of the studied deposit and represents perhaps one of the most dangerous possible scenarios of the Copahue volcanic activity. PDCs occurrence has been considered in the last volcanic hazards map as a low probability process; evidences found in this contribution suggest instead to include them as more probable and thus very important for the hazards assessment of the Copahue volcano.

Keywords: Copahue, Hazards assessment, Southern Volcanic Zone, Andes, Cavihue, active volcanism

1. Introduction

The Southern Volcanic Zone (SVZ) of the Andes (33°- 46° S) is the result of the subduction of the Nazca plate beneath the South American plate (e.g. Stern et al., 2007). It includes several Quaternary stratovolcanoes, large volcanic fields and calderas, as well as hundreds of monogenetic volcanoes.

The Cavihue-Copahue Volcanic Complex (Pliocene to present) is located in the Central SVZ (CSVZ), the widest segment of the SVZ arc (e.g. Lara 2001; Stern et al., 2007) that develops between 34.4° S and 39.5° S (Fig. 1a). It comprises the Cavihue/Agrio caldera and the post-caldera Copahue volcano (Fig. 1b) located in its southwestern margin (Mazzoni and Licitra, 2000; Varekamp et al., 2006 and references therein). The Pleistocene to Holocene Copahue volcano (37° 51' S, 71° 10' W) is an active polygenetic stratovolcano, with basaltic to andesitic composition and shield morphology (Delpino and Bermúdez, 1993; Naranjo and Polanco, 2004). It has nine summit craters aligned at N60°E; the easternmost is the currently active one (Fig. 1c), hosting an ephemeral acid crater-lake outlined by hot springs, which are fed by a 1500 m deep hydrothermal system (Varekamp et al., 2001; 2009).

The volcanic potential hazards map for Copahue (Naranjo et al., 2000) includes areas with high to moderate probability of being affected by lavas and/or lahars and areas with very low probability of occurrence of 0.1 to 1 km³ pyroclastic flows. Polanco (2003) suggests that the major volcanic risk of the Copahue volcano are lahars that could affect the people living near the river canyons, as Cavihue town (Fig. 1b), but mentioned 6 pyroclastic deposits dated between 8770 and 2200 BP including ash-flow tuffs, surge and ash-fall deposits. Additionally, Naranjo and Polanco (2004) mentioned pyroclastic surges associated with the 2000 AD eruption. Similarly, the initial

explosions of the 2012 AD eruption produced several pyroclastic flows from the E border of the actual crater, that flowed through the Agrio river (Caselli et al. 2015a, Fig. 4.7); apparently there are no preserved records of its deposits. The only geological record of pyroclastic flows deposits is the one documented by Petrinovic et al. (2014a) along the eastern slope of the volcano, interpreted as formed by the 1961 AD eruption and assumed as the most recent and dangerous potential hazard.

In this contribution we focused on the latter deposit, for which the determination of the appropriate age and distribution is essential for the hazards assessment related with the activity of the Copahue volcano. We thus present sedimentological, petrographic and facies analyses and discuss the age proposed by Petrinovic et al. (2014a) for the deposit located in the margins of Arroyo Dulce, Agrio and Lomín rivers (Fig. 2) in order to interpret its eruptive mechanisms, its age and its depositional conditions.

2. The Holocene eruptions of the Copahue volcano

The Holocene activity of the Copahue volcano is poorly known (Caselli et al., 2015b). There are mentions of phreatic and phreatomagmatic activity with the generation of fallout tephra, pyroclastic flow deposits and lahars (Polanco et al., 2000; Polanco, 2003; Stern et al., 2007).

Thirteen phreatic to phreatomagmatic historical eruptions have been reported for this volcano in the last centuries (Naranjo and Polanco, 2004; Global Volcanism Program, 2013), but only the ones of 1992 AD, 2000 AD and 2012 AD were described in detail (Delpino and Bermúdez, 1993; Naranjo and Polanco, 2004; Petrinovic et al., 2014b). These three last eruptions were phreatic and phreatomagmatic, had a VEI < 2, with eruption columns that reached < 3 km. However, all the historical records were interpreted to have produced mainly ballistic ejecta, fallout tephra, lahar deposits and

probably small pyroclastic density currents (e.g. Polanco, 2003; Naranjo and Polanco, 2004).

The 1992 AD (VEI 1-2) eruption was the most long-lasting of the recent ones (July 1992-August 1993), forming a 0.3 to 1.4 km-high eruptive column (Delpino and Bermúdez, 1993). The products associated with this eruption (Delpino and Bermúdez, 1993; Polanco, 2003; Sruoga and Consoli, 2011) include: i) lahar deposits with predominantly ash grain-size, located in the margins of the Agrio and Lomín rivers; ii) ballistic ejecta that frequently contain sulphur (liquid at the moment of the impact).

The 2000 AD and 2012 AD eruptions (VEI ≤ 2) were characterised by a pulsating eruptive column of 1.5 to 3 km-high accompanied by the emission of SO₂ (Naranjo and Polanco, 2004; Petrinovic et al., 2014b). Particularly, the 2000 AD eruption was characterised by five eruptive cycles (Naranjo and Polanco, 2004), with sulphur particles, ash and highly vesicular bombs, accessory fragments including white to grey quartz (from the walls of the conduit) and gas (mainly SO₂). Small-volume pyroclastic surges, mudflows and floods, ash-fall and ballistic bombs were the common process and products of this eruptive cycle (Naranjo and Polanco, 2004).

The 2012 AD eruption was characterised by proximal ballistic blocks (hydrothermally altered volcanic and subvolcanic rocks), unaltered bombs and ash-fall deposits in proximal to distal facies (Petrinovic et al., 2014b).

3. Methodology

Field work included sampling (AGR# prefix) and conventional physical volcanology observations and measurements (colour, morphology, thickness, sedimentary structures, principal components and particle size in all the surveyed sections).

Laboratory tasks included sieve analysis by sieving and by laser diffraction with a LA-960 Laser Particle Size Analyser. The components were analysed by binocular loupe in the LabGeo laboratory, confocal microscopy and Scanning Electronic Microprobe (SEM) in the LAMARX laboratories, Universidad Nacional de Córdoba, Argentina. Confocal microscopy images were obtained with an OLYMPUS LEXT OLS4000 microscope, with a 405 nm laser and a spatial resolution of 10 nm. SEM images were obtained in a FE-SEM Sigma microscope with a Schottky system and EDS, WDS, EBSD spectrometers. Deposit density (for DRE computation) was calculated using an approximation of magma density by its composition and vesiculation degree.

The lithofacies were described using the terminology and abbreviations suggested by Branney and Kokelaar (2002).

In order to simulate the pyroclastic flow and initial conditions we used the freeware Volcflow© (Kelfon, 2015) using a SRTM 30-m digital elevation model (DEM). Input variables for this program are: initial volume of material to model (km^3); time between pulses (s); maximum time for the calculation (s); internal friction angle (rad) and external friction angle (rad); gravity (m/s^2); density -rho- (kg/m^3); cohesion (Pa) and viscosity (Pa s).

4. Characteristics of the 2000/1961 AD pyroclastic flow deposit

The studied deposit is whitish grey, 10-40 cm thick and 5-6 km long, confined approximately along the Agrio and Lomín rivers (Figs. 1 and 2). Thickness and distribution inside the canyons are controlled by topographic features, so that the deposit is thin and narrow in sections with high slope, whereas in the flattest sections (solid red stars in Fig. 1c) it thickens and expands. In the segments of the canyons with the steepest slope, deposits lay both at the bottom of the valley and above fluvial

terraces. Those at the terraces do not show the typical internal characteristics of veneer deposits (Brown and Branney, 2013) because they are very thin (less than few centimetres) or were eroded. One remarkable feature observed in this deposit is that it contains charred bushes, lying in the flow direction (Fig. 3).

The deposits cover an area of 1.15 km² (Fig. 1c) with an average thickness of 0.2 m. We estimated a total volume of 0.00012 km³ using *Dense Rock Equivalent (DRE)* = [*tephra volume***tephra density* / *magma density*]. The preservation of the deposit is expected to be low due to weather conditions of the region. During the 2007-2015 AD period, we observed that much of these outcrops disappeared or were reduced significantly, especially those in the flat zones. Therefore, the original deposit may have covered much greater areas and had greater volumes than the present one.

4.1. Petrography of the components

The components of the deposit are 10% vesicular glassy fragments and 90% non-glassy fragments; this ratio is constant among the outcrops at all surveyed sections.

Vesicular glassy fragments are differentiated on the basis of their vesicles content in a group of 90 vol. % of vesicles (Fig. 4a) and a group with 20 vol. % of vesicles (Fig. 4b). Both groups of glassy fragments show grain sizes ranging from 0.2 cm to 3 cm, they contain tabular plagioclase and pyroxene crystals set in a glassy groundmass and are characterised by regularly flattened vesicles as observed with confocal microscopy (Figs. 4c, d) and SEM (Figs. 4e, f). Vesicles have diameters of 255 µm or less (Figs. 4c, d) and in some cases coalesce forming reticulites (Fig. 4b). The vesicle walls are often fractured with radial patterns (Figs. 4d, e, f) and commonly filled with whitish sulphates with saccharoidal aspect (alunite – jarosite?) and silicates (as shown in Fig. 5) which are common minerals in Copahue spring fluids (Varekamp et al., 2014). The vesicular

glassy fragments with 90% of vesicles are usually filled by sulphates (Fig. 5a), whereas in those with 10% of vesicles Si/S is higher, thus indicating a prevalence of silicates infill (Fig. 5b).

The non-glassy fragments differ substantially from vesicular glassy ones; we distinguish: i) greyish-green rounded clasts of a volcanic fragment (Fig. 6a) ranging from 0.01 to 1.5 cm across, with vesicles smaller than 1 mm filled by native sulphur; ii) whitish subrounded hydrothermal clasts (Fig. 6b), ranging from 0.01 to 2 cm, composed of silica and sulphates (alunite-jarosite?) with saccharoidal texture and iii) reddish and subrounded volcanic clasts (Fig. 6c) ranging from 0.02 to 1 cm, with saccharoidal appearance and plagioclase crystals.

Since all the components do not differ neither in nature nor in percentage in all the surveyed sections, the criteria to distinguish two lithofacies is based on a marked wavy contact between them and is evidenced by varying grain-size of the components, stratification and fabric.

4.2. Lithofacies

4.2.1. sT Facies (*Stratified and cross-stratified tuffs*)

This lithofacies is whitish grey with thickness ranging from 3 to 15 cm. It has a well-defined slightly wavy base and it is covered by the mLTI facies (see below) with a wavy contact (Fig. 1c). This facies is laminated in sets of ≈ 1 cm with parallel and cross stratification (Figs. 7a, b). Upwards, the lamination becomes diffuse and is characterised by tilted and folded sets (Figs. 7a, b). The grain-size of the components varies from extremely fine ash to medium ash (≥ 0.004 mm to ≤ 0.5 mm: after White and Houghton, 2006) (Fig. 8a). This facies is usually found in areas with gentle slopes within the Agrio canyon (AGR 1, AGR 3 and AGR 7: Fig. 9).

4.2.2. mLTI Facies (*massive lapilli-tuff lithic-rich*)

Light grey in colour, 10 to 40 cm in thickness and a well-defined flat to wavy base, with poor sorting of the components (Figs. 7a, c). This facies overlies the sT lithofacies (Fig. 1c) or is above older volcanic deposits of the Copahue volcano. Lens-shaped structures of mLTI facies are found within the sT facies with semi-flat bases and convex tops of 20 cm across and 5 cm thick (Fig. 7c).

The matrix is fine ash with clasts/matrix ratio less than 0.4. The grain size of the components varies from extremely fine ash up to coarse lapilli (≥ 0.015 mm to ≤ 30 mm), but the lapilli size prevails (Fig. 8b). This facies is found in all the surveyed sections (Fig. 9).

5. Interpretation

5.1. *Pre-eruptive conditions*

Vesiculation degree and shapes of vesicles of the glassy fragments indicate their juvenile nature, which show a persistent mineralogy in all the fragments. The non-glassy and mineralogically heterogeneous fragments are interpreted as accessory fragments. The latter belong to the Copahue edifice (<1000 m high) and/or to the caldera infill (>2000 m thick), so it is not possible to constrain the depth where they come from.

The characteristics of the juvenile fragments such as vesicle percentage (20 to 90 %), fractured vesicles walls and filled vesicles, and the nature of the accessory fragments allow us to interpret the succession of events from the pre-eruptive stages. The difference in vesicle percentage in the two groups of juvenile fragments is interpreted to be related to variable conditions during the ascent of the melt through the conduit,

including rising levels of disruption and increasing degree of gas saturation in the melt (e.g. Németh and Ulrike, 2007). As deduced from the fractured vesicles walls, vesiculation was attained before the incorporation of water (Figs. 4d, e, f). These brittle fractures were generated by sudden contraction of the vesiculated melt in contact with water (Büttner et al., 2002) from the hydrothermal system of Copahue volcano. The same hydrothermal liquids enriched in SO₂ and other volatiles (Fig. 5) induced the precipitation of sulphates into the vesicles. According to Varekamp et al. (2009) this hydrothermal system is located at 1500 m below the surface, where the interaction of vesiculated magma with the hydrothermal system may have occurred. Additionally, Velez et al. (2011) interpreted the magma reservoir to be located at ~4,000 m deep (see Fig. 8 in Velez et al., 2011). Therefore, the vesiculation of magma occurred at any depth between 1500 m and 4000 m.

This depth of vesiculation and fragmentation level may be constant in depth in different phreatomagmatic eruptive cycles, as described by Petrinovic et al. (2014b) in the 2012 AD eruption.

5.2. PDCs characteristics

Most of the previous contributions consider that deposits from the recent (>250 years) activity of the Copahue volcano were ballistic ejecta, fallout tephra and lahar deposits. For example, Delpino and Bermúdez (1993) describe “pyroclastic sulphur” in the 1992 AD eruption, in the form of native sulphur inside ballistic clasts. Polanco (2003) reported the occurrence of lahar flows during the eruption of July and August 1992 AD; it is interesting that the pattern of distribution of that deposit is similar to the deposit studied in the present contribution. Sruoga and Consoli (2011) interpreted the same

deposit that we described, as produced by a lahar (see Fig. 6c in Sruoga and Consoli, 2011), but mentioned the existence of “base surges”.

Taking into account the field and analytical evidences and according to the lithofacies analysis and their association, we interpret the deposit as sedimented from pyroclastic density currents that were diluted at the base, and concentrated at the top, resulting in deposits similar to the ones described by Dellino et al. (2004a, b) in Agnano Monte Spina eruption.

Field evidences supporting this interpretation are: i) the presence of charred and lying down bushes in both Agrio and Lomín valleys (Fig. 3); ii) the presence of the deposit adhered to the bends of the Agrio channel (15 m above the valley floor, which is only possible with highly cohesive particles supported by gas); iii) two lithofacies with the same components evidencing a progressive and vertical aggradation; and iv) the persistence of juvenile components with the same characteristics along the entire deposit.

A lahar, even a “hot lahar” (commonly used to describe hot debris flows coeval with eruptions) produces a poorly sorted and massive deposit that fills the entire section of the river valley, with common debris avalanche deposits associated with lahar dams (e.g. Waythomas, 2001). “Hot lahars” are derived from a primary pyroclastic deposit upstream, or from the instability of tephra accumulations around the vent. The latter is the case of small lahars associated to the 1992 AD eruption (from the oral reports of the residents of Caviahue), composed by dark subrounded vesicular clasts and whitish subangular blocks of 10 cm in diameter. These clasts were previously accumulated around the vent as bombs and ballistic ejecta and were later transported downstream (Fig. 10), thus consisting of small debris flows or lahars that were formed by a quick

accumulation of unstable debris and snowmelt (in winter, a thick pile of snow covers the volcano).

At first, the PDCs flowed widely and quickly through the NE-SE slopes of the Copahue volcano, producing the sT lithofacies forming very thin layers (few centimetres) in proximal areas and slightly thicker ones in the river valleys (Río Agrio and Río Lomín in Fig. 9). Today, most of the records of this lithofacies are missing because of erosion; they were only preserved inside the valley channels when covered by the mLTI lithofacies. This pattern of distribution of the sT combined with its stratified nature is indicative of an explosive opening of conduits with high proportion of steam. Hence, diluted and very fast PDCs were generated, with a traction-dominated flow-boundary zone (possibly associated with a shock wave). After that, denser PDCs with a granular flow-dominated flow-boundary zone were confined into the valleys of Agrio and Lomín rivers (Fig. 2) and progressively deposited the mLTI facies. The lens of mLTI within the sT facies are interpreted as formed by reduced and localised dense PDCs, interfingering with the more diluted ones. A similar case was described by Palladino and Simei (2002), who described a continuum of pyroclastic currents ranging from dilute to concentrated end members in the Vulsini Volcanic District (central Italy).

None of the lithofacies shows grading (Fig. 9) while an upwards and lateral gradual decrease of particle sizes would be expected in the flow direction (Bursik and Woods, 1996). The presence of components smaller than 0.025 mm within the mLTI facies was observed at places where the sT facies was not preserved, thus (Fig. 8b) we interpret that these small particles were incorporated from the previously deposited sT facies.

The lack of weathering surfaces between both facies, the identical characteristics of their components and the presence of mLTI as lenses inside the sT facies, are evidences

of a continuous and sustained eruption in time. The vertical association between facies responds to changes in the eruptive dynamics, from a diluted to a denser column by increment of the proportion of solid particles due to enlargement of the conduit diameter and/or variations in the level of fragmentation/water incorporation (De Rosa et al., 1992; Palladino and Simeì, 2002). The first hypothesis is preferred due to the fact that the water involved in this eruption came from a hydrothermal system whose depth is considered stable at ca. 1500 m depth. This in turn, modified the flow regime of the PDC and the progressive aggradation of the PDCs from turbulent to laminar flow.

Thus, the sT facies represent the opening of conduit and the formation of a diluted and short-lived eruptive column that was inclined eastwards. As observed in the last eruptive episodes (1992-2000 AD and 2012 AD), the typical eruptive dynamics of this volcano rarely form columns higher than 1000-2000 m. At the same eruptive rate, the percentage of components were proportionally increased by conduit-widening, as is commonly observed in phreatomagmatic eruptions (Doubik and Hill, 1999), which promoted the immediate collapse of the column with PDCs forming the mLTI facies. In some areas, dense PDCs eroded the dilute ones and covered them. This may explain the fine-grained particles incorporation in the dense PDCs and the slightly waved contact between both facies.

The lack of detailed Holocene volcanic stratigraphy (Caselli et al., 2015b) and the frequent mention of phreatomagmatic eruptions in the last Copahue volcano records (Delpino and Bermúdez, 1993; Naranjo and Polanco, 2004; Petrinovic et al., 2014b) indicate that our proposed occurrence of PDCs is not a rare phenomenon in the Copahue activity.

Phreatomagmatic to phreatic eruptions are common in Andean volcanoes (e.g. Solipulli: Lachowycz et al., 2015; Maipo: Sruoga et al., 2005; Mocho-Choshuenco: Rawson et al., 2015; Puyehue-Cordon Caulle: Lara et al., 2006; Peteroa: Haller and Risso, 2011; Payunia: Risso et al., 2009, among others). The origin of water could be from glaciers, snow, phreatic waters and hydrothermal systems, and most of the SVZ polygenetic volcanoes have one or more of these elements associated. The most dangerous situation is when hydrothermal systems interact with the magma reservoir, because of the water state. The superheated liquid water is the most efficient state to produce vigorous explosions; the presence of non-vaporizable components in solution (silica, sulphur, chlorine) and sediments in suspension increases density and viscosity of the mixture and decreases the heat transfer capacity (Sigurdsson et al., 2015). This is the case of the last phreatomagmatic eruptions at Copahue volcano (including the one studied here), where superheated and sulphur-rich waters at depth interact with magma.

6. Age

In Petrinovic et al. (2014a) two possible ages are proposed for this deposit: 1963-1964 AD and 1976 AD. However, considering the range of possibilities of the radiocarbon age of Petrinovic et al. (2014a) and because of the nature of the sample (*Nothofagus*: Donoso, 1987), the obtained age may be slightly older than the real one because of the incomplete charring of the wood.

A minor eruption in 1961 AD was mentioned by Naranjo and Polanco (2004) with at least two successive phreatic explosions, but there are no reports of pyroclastic flows or a significant eruption that may have caused PDCs. Therefore, it is difficult to relate the magnitude of the process here interpreted, with the characteristics of the 1961 AD eruption. Delpino and Bermúdez (1993), Polanco (2003) and Sruoga and Consoli

(2011), report lahar deposits related to the 1992 AD eruption at the E and SE volcano slopes that have similar components and characteristics as the ones described here. If this is the same deposit, and with the arguments presented above, the characteristics of the lithofacies cannot be explained by lahar processes. Naranjo and Polanco (2004), described in great detail the 2000 AD eruption, and mentioned pyroclastic surges at the first stage of the eruption: on July 5th, affecting the N and E flanks of the volcano, as well as formation of lahars that flowed through the Agrio creek on July 7th. Moreover, oral reports of people from Caviahue, confirm the occurrence of approximately hourly strong explosions on July 5th and the onset of a whitish and thin deposit in the Lomín and Agrio rivers during those days. Thus, given the characteristics, persistence in time and intensity of the 2000 AD eruption, short-lived pyroclastic density currents may have occurred on July 5th. Hence, we interpret that the deposit studied in the present contribution might have been formed during the 2000 AD eruption.

7. Simulation of pyroclastic flow distribution

In order to infer the possible initial conditions and physical variables that controlled the PDCs, we simulated 20 models with different variables using the freeware Volcflow© (Kelfon, 2015) and a Digital Elevation Model. We considered an initial volume of material similar to the studied deposit (0.002 km^3). The maximum time for the calculation was set at 400 s, internal friction angle and external friction angles were assumed to be zero, density was assumed to be 2000 kg/m^3 . We then used a range of cohesion values from 2500 to 25000 Pa and a range of viscosity from 10^2 to 10^7 Pa s. With these variables we selected two extreme models: i) a “dense” model with a cohesion of 25000 Pa and a viscosity of 10^7 Pa s, which formed a locally distributed deposit around the vent (Fig. 11a); ii) a “more diluted” model with a cohesion of 2500

Pa and a viscosity of 10^2 Pa s (Fig. 11b), which produced material channelised in fluvial canyons, and represents the most dangerous scenario (Fig. 11b).

8. Hazards assessments implications

The combination of variables as: i) the age of the last PDC forming process (2000 AD) with evidences of high temperatures, ii) the presence of several towns around the volcano flanks, iii) the high slopes of the volcano flanks and iv) the repeated occurrence of eruptions of phreatomagmatic nature at Copahue volcano in the last centuries, gives the possibility to estimate a possible scenario of hazard to be considered in assessing the Copahue volcanic risk.

The most affected areas in case of a PDC forming process would be the villages around the volcano as Trapa Trapa (13 km to the NW), Caviahue (10 km to the E), Guallalí (25 km to the SW) and Copahue (7 km to the NE), located in the river beds of Llai, Queuco, Agrio and Lomín rivers and Dulce stream (Fig 1b).

Specifically, the Agrio river and Dulce stream (in the sky resort area: Fig. 1) are the most affected areas in our modelling results. The PDC can reach the Caviahue town if necessary conditions are achieved, both through the Agrio river and from the Dulce stream (Fig. 11b).

These implications reinforce the need for the update of the hazards assessment of the Copahue volcano, as highlighted by its 9th position in the ranking of the active Chilean volcanoes (SERNAGEOMIN 2016).

9. Conclusions

Given the evidences in terms of temperature, field relationships, characteristics of the components and facies and their arrangement, it is possible to characterise the analysed

deposit as a recent PDC produced by a phreatomagmatic eruption. We suggest the 2000 AD age for this deposit, because of its characteristics and the oral reports from the Caviahue inhabitants.

Vesiculation occurred at a depth between 4000 m and 1500 m. The interaction of magma with water and steam of the hydrothermal system (above 1500 m depth) increased the explosiveness of the eruption ($VEI \leq 2$, based on volume of the deposit) and promoted fragmentation of magma (formation of vesicular juvenile fragments) and fracturing of the volcanic wall rock (formation of accessory fragments); finally volatiles rich in sulphur filled the vesicles of those fragments.

The conduits were opened by the initial explosion that generated a high-speed diluted PDC possibly associated with a shock wave. After that, a dense PDC was formed by a low-altitude and dense column resulting from the increased diameter of the conduit incorporating a higher proportion of accessory fragments. Moreover, the facies architecture formed by a *stratified tuff* (sT) facies at the base, followed by an upper *massive lapilli tuff* (mLTI) facies would reverse the classical model of progressive aggradation, supporting the change in the interpreted eruptive regime. The lens of mLTI facies inside the sT ones represents dense PDC's formed by openings of minor conduits, which would confirm the concurrence of both processes at approximately the same time.

The occurrence of similar accessory fragments in more recent eruptions (i.e. 2012), suggests that the fragmentation level is constant in the Copahue volcano in the last decades.

PDCs occurrence has been considered to have a very low probability in the available volcanic hazards map, but the existence of processes such as the ones interpreted here are relevant for the hazards and risk assessment of the Copahue volcano.

Acknowledgements

This work was funded by PICT Raíces 265 and DFG-CONICET International Cooperation Program (2015). We thank Gustavo Villarosa, Roberto Carniel, Raquel Villegas, Cecilia del Papa, Leandro D'Elía, Gerardo Páez and Ulrich Riller for their contributions at fieldwork. Special thanks to G. Kereszturi and an anonymous reviewer that helped improving the quality of the first version of this manuscript.

References

Branney, M. J., Kokelaar, P., 2002. Pyroclastic density currents and the sedimentation of ignimbrites. Geol. Soc. London, United Kingdom.

Brown, R. J., Branney, M. J., 2013. Internal flow variations and diachronous sedimentation within extensive, sustained, density-stratified pyroclastic density currents flowing down gentle slopes, as revealed by the internal architectures of ignimbrites on Tenerife. Bull. Volcanol. 75 (7), 1-24.

Bursik, M. I., Woods, A. W., 1996. The dynamics and thermodynamics of large ash flows. Bull. Volcanol. 58 (2-3), 175-193.

Büttner, R., Dellino P., La Volpe, L., Lorenz, V., Zimanowski, B., 2002. Thermohydraulic explosions in phreatomagmatic eruptions as evidenced by the comparison between pyroclasts and products from Molten Fuel Coolant Interaction experiments. J. Geophys. Res. 107 (B11), ECV 5-1–ECV 5-14.

Caselli, A.T., Agosto, M., Velez, M. L., Forte, P. Bengoa, C. Daga, R., Albite, J.M. and Capaccioni, B., 2015a. The 2012 eruption. In: Tassi, F., Vaselli, O., Caselli, A.T., (Eds.), Copahue Volcano. Active volcanoes of the World. Springer Verlag, Berlin, pp. 61-77.

Caselli, A.T., Velez, M. L., Agosto, M., Liccioli, C. and Vaselli, O., 2015b. Prehistoric to historic volcanic activity at Copahue volcano. In: Tassi, F., Vaselli, O., Caselli, A.T., (Eds.), Copahue Volcano. Active volcanoes of the World. Springer Verlag, Berlin, pp. 49-59.

Delpino, D., Bermúdez, A., 1993. La actividad del volcán Copahue durante 1992. Erupción con emisión de azufre piroclástico. Provincia de Neuquén-Argentina. XII Congreso Geológico Argentino y Segundo Congreso de Exploración de hidrocarburos, Mendoza, Actas 4, pp. 292-301.

Dellino, P., Isaia, R., La Volpe, L., Orsi, G., 2004a. Interaction between particles transported by fallout and surge in the deposits of the Agnano–Monte Spina eruption (Campi Flegrei, Southern Italy). *J. Volcanol. Geotherm. Res.* 133 (1), 193-210.

Dellino, P., Isaia, R., Veneruso, M., 2004b. Turbulent boundary layer shear flows as an approximation of base surges at Campi Flegrei (Southern Italy). *J. Volcanol. Geotherm. Res.* 133(1), 211-228.

De Rosa, R., Frazzetta, G., La Volpe, L., 1992. An approach for investigating the depositional mechanism of fine-grained surge deposits. The example of the dry surge deposits at “La Fossa di Vulcano”. *J. Volcanol. Geotherm. Res.* 51(4), 305-321.

Donoso, C., 1987. Variación natural en especies de *Nothofagus* en Chile. *Bosque*, 8 (2), 85-97.

Doubik, P., Hill, B.E., 1999. Magmatic and hydromagmatic conduit development during the 1975 Tolbachik Eruption, Kamchatka, with implications for hazard assessments at Yucca Mountain, NV. *J. Volcanol. Geotherm. Res.* 91 (1), 43-64.

Global Volcanism Program, 2013. Report on Copahue (Chile-Argentina). In: Wunderman, R., (Ed.), *Bulletin of the Global Volcanism Network*, Smithsonian Institution. 38:9. <http://dx.doi.org/10.5479/si.GVP.BGVN201309-357090>.

Haller, M. J., Risso, C., 2011. La erupción del volcán Peteroa (35°15' S, 70°18' O) del 4 de septiembre de 2010. *Rev. Asoc. Geol. Arg.* 68 (2), 295-305.

Kelfon, K., 2015. Simulation of volcanic flows. VolcFlow: http://wwwobs.univ-bpclermont.fr/lmv/pperm/kelfoun_k/VolcFlow/VolcFlow.html.

Lachowycz, S. M., Pyle, D. M., Gilbert, J. S., Mather, T. A., Mee, K., Naranjo, J. A., Hobbs, L. K., 2015. Glaciovolcanism at Volcán Sollipulli, southern Chile: Lithofacies analysis and interpretation. *J. Volcanol. Geotherm. Res.* 303, 59-78.

Lara, L., Rodríguez, C., Moreno, H., Pérez de Arce, C., 2001. Geocronología K-Ar y geoquímica del volcanismo plioceno superior-pleistoceno de los Andes del sur (39-42 S). *Rev. Geol. Chilena* 28(1), 67-90.

Lara, L. E., Moreno, H., 2006. Geología del Complejo Volcánico Puyehue-Cordón Caulle. Región de Los Lagos, Chile. Carta geológica de Chile, Serie Geología Básica n° 99, DOI: 10.13140/RG.2.1.4531.2886.

Mazzoni, L. A., Licitra, D. T., 2000. Significado estratigráfico y volcanológico de depósitos de flujos piroclásticos neógenos con composición intermedia en la zona del lago Caviahue, Provincia del Neuquén. *Rev. Asoc. Geol. Arg.* 55 (3), 247-249.

Naranjo, J. A., Polanco, E., 2004. The 2000 AD eruption of Copahue Volcano, Southern Andes. *Rev. Geol. Chile* 31(2), 279-292.

Naranjo, J. A., Moreno, H., Polanco, E., Young, S., 2000. Mapa de peligros de los volcanes del Alto BioBio. Servicio Nacional de Geología y Minería, documentos de trabajo 15.

Németh, K., Ulrike, M., 2007. Practical volcanology. Occasional Papers of the Geological Institute of Hungary, 207, pp. 220.

Palladino, D. M., Simei, S., 2002. Three types of pyroclastic currents and their deposits: examples from the Vulsini Volcanoes, Italy. *J. Volcanol. Geotherm. Res.*, 116 (1), 97-118.

Petrinovic, I. A., L. D'Elia, G. Páez, C. Balbis, S. Guzmán, G. Villarosa, R. Carniel., 2014a. Depósito de corriente piroclástica reciente (1963-64 AD?-1976 AD?) del volcán Copahue (I): evidencias geológicas de campo y edad radiocarbónica. *Rev. Asoc. Geol. Arg.* (1), 140-143.

Petrinovic, I. A., Villarosa, G., D'Elía, L., Guzmán, S. P., Páez, G.N., Outes, V., Manzoni, C., Delmónico, A., Balbis, C., Carniel, R., Hernando, I. R., 2014b. La erupción del 22 de diciembre de 2012 del volcán Copahue, Neuquén, Argentina: caracterización del ciclo eruptivo y sus productos. *Rev. Asoc. Geol. Arg.* 71 (2), 161-173.

Polanco, E., Naranjo, J. A., Young, S., Moreno, H., 2000. Volcanismo Explosivo Holoceno en la Cuenca del Alto Biobío, Andes del Sur (37 45'-38 30'S). 9º Congreso Geológico Chileno, Puerto Varas, Chile, 2, pp. 59-61.

Polanco, E., 2003. Evolución del volcán Copahue (37 45'S), Andes del Sur. Master thesis, Universidad Autónoma de Mexico, pp. 103.

Rawson, H., Naranjo, J. A., Smith, V. C., Fontijn, K., Pyle, D. M., Mather, T. A., Moreno, H., 2015. The Frequency and Magnitude of Post-Glacial Explosive Eruptions at Volcán Mocho-Choshuenco, Southern Chile. *J. Volcanol. Geotherm. Res.* 299, 103-129.

Risso, C., K. Németh, F. Nullo., 2009. Field Guide Payún Matru and Llancanelo Volcanics Fields, Malargüe - Mendoza. 3rd International Maar Conference, Malargüe, Argentina, pp. 28.

SERNAGEOMIN, 2016. Ranking de los 90 volcanes activos de Chile – SERNAGEOMIN. www.sernageomin.cl/archivos/Ranking-de-Volcanes.pdf.

Sigurdsson, H., Houghton, B., McNutt, S., Rymer, H., Stix, J., 2015. *The Encyclopedia of Volcanoes II Ed.*, Elsevier, Amsterdam.

Stern, C. R., Moreno, H., López-Escobar, L., Clavero, J. E., Lara, L. E., Naranjo, J. A., Parada, M. A., Skewes, M. A., 2007. Chilean volcanoes. In: Moreno, T., Gibbons, W. (Eds.), *The Geology of Chile*. Geological Society of London, London, United Kingdom, pp.149-180.

Sruoga, P., Consoli, V., 2011. Volcán Copahue. In: (Leanza, H.A., Carbone, O. Arregui, C., Vallés, J.M. (Eds.)), *Geología y Recursos Naturales de la provincia del Neuquén, Relatorio 18° Congreso Geológico Argentino*. Neuquén, Argentina, pp. 613-621.

Sruoga, P., Etcheverría, M., Folguera, A., Repol, D., Cortes, J. M., Zanettini, J. C., 2005. Hoja Geológica 3569-I Volcán Maipo, Provincia de Mendoza. Instituto de

Geología y Recursos Minerales, Servicio Geológico Minero Argentino, Boletín no. 290, pp. 92.

Varekamp, J. C., Ouimette, A. P., Herman, S. W., Bermúdez, A., Delpino, D., 2001. Hydrothermal element fluxes from Copahue, Argentina: a “beehive” volcano in turmoil. *Geology* 29 (11), 1059-1062.

Varekamp, J. C., Maarten de Moor, J., Merrill, M. D., Colvin, A. S., Goss, A. R., Vroon, P. Z., Hilton, D. R., 2006. Geochemistry and isotopic characteristics of the Caviahue-Copahue volcanic complex, Province of Neuquén, Argentina. *Geol. Soc. of Am. Sp. Papers* 407, 317-342.

Varekamp, J. C., Ouimette, A. P., Herman, S. W., Flynn, K. S., Bermudez, A., Delpino, D., 2009. Naturally acid waters from Copahue volcano, Argentina. *App. Geochem.* 24 (2), 208-220.

Varekamp, J. C., Ouimette, A. P., Kreulen, R., 2014. The magmato-hydrothermal system at Copahue volcano, Argentina. *Water–Rock Interaction.* 11, 215-218.

Velez, M. L., Euillades, P., Caselli, A., Blanco, M., Díaz, J. M., 2011. Deformation of Copahue volcano: Inversion of InSAR data using a genetic algorithm. *J. Volcanol. Geotherm. Res.* 202, 117-126.

Waythomas, C.F., 2001. Formation and failure of volcanic debris dams in the Chakachatna River valley associated with eruptions of the Spurr volcanic complex, Alaska. *Geomorphology* 39, 111–129.

White, J. D. L., Houghton, B. F., 2006. Primary volcaniclastic rocks. *Geology*, 34 (8), 677-680.

Figure captions

Fig. 1. (a) Location of the Volcanic Zones of the Andes of South America. (b) Position of the Cavihue-Copahue Volcanic Complex. (c) Distribution of lithofacies (after Petrinovic et al. 2014a) described in this contribution: mLTI facies in light brown and sT facies outcrops indicated by solid red stars. Pink diamond indicates places where charred bushes were found.

Fig. 2. Distribution of the deposit, red arrows indicate flow direction. (a) Towards the E-ESE by the Agrio river. Photo taken at $37^{\circ} 51' 8.95''$ S / $71^{\circ} 07' 7.18''$ W. (b) Towards the SSE through a flat area of the Río Lomín valley. Photo taken at $37^{\circ} 52' 53.68''$ S / $71^{\circ} 8' 11.13''$ W. The scales represent the nearest image plane.

Fig. 3. Charred bushes and their alignment indicating the flow direction of the mLTI lithofacies. Photo taken on the banks of the Agrio river (see Fig. 1c).

Fig. 4. Detailed photographs of juvenile components. (a) and (b) images taken with binocular loupe (see text for explanation). (c) and (d) images from confocal microscopy. (c) Flattened shape of vesicles filled by sulphates. (d) Detail of the cracks on vesicles surface (enclosed by a solid yellow line); acicular crystals are secondary gypsum. (e) - (f) Images from SEM of juveniles clasts. Images showing the cracks on the vesicles (enclosed by a solid yellow line) and their filling by saccharoidal sulphates apparently precipitated after the fractures. In (d) the fracture is well developed on the middle of the image. (a), (c), (e) clasts of AGR 1 section. (b), (d), and (f) clasts of AGR 11 section (see Fig. 9).

Fig. 5. SEM images of filled vesicles. As indicated in the semi-quantitative analyses in both images (by EDS), the material refilling vesicles is a mixture of sulphates of Al, Na, Fe and silicates (or silica). In the (a) case, sulphates are minor in content, increasing in

the (b) case in relation with better developed vesiculation. Clasts of AGR 1 and AGR 11 sections (see Fig. 9). The obtained spectra from EDS was normalized to get rid of the background noise.

Fig. 6. Detailed photographs taken with binocular loupe of the accessory components Clasts of AGR 4 section (see Fig. 9)

Fig. 7. Stratigraphic relationships of lithofacies at AGR 5 section (see Fig. 9). (a) The sT facies below the mLTl ones and their bulk characteristics. (b) Detail of (a) showing the parallel and cross stratification of sT facies. (c) Lens of mLTl facies into the sT ones as described in the text. Dotted lines mark the facies contact, solid white lines indicate the base of sT facies and solid black lines indicates the lamination.

Fig. 8. Grain-size distributions with relative abundances of the different fractions for samples at the AGR 5 profile for (a) sT facies and (b) mLTl facies.

Fig. 9. Distribution and surveyed sections of the deposit (as in Fig. 1). Stratigraphic sections: Vertical scale in vertical B&W rectangles (10 cm each); (fa) Fine ash, (la) Lapilli. Correlation of the mLTl base in red line.

Fig. 10. Photograph of lahars viewed from Caviahue town towards the western slope of the volcano, few days after the 1992 eruption (credit from Higinio del Monte).

Fig. 11: VolcFlow© models. (a) “Diluted” model (see text for explanation of variables) reproduces the deposit distribution. (b) “Dense” conditions, the deposits are immediately accumulated around the vent. Colours indicate the thickness of the modelled deposit, from red (thickest) to blue (thinnest).

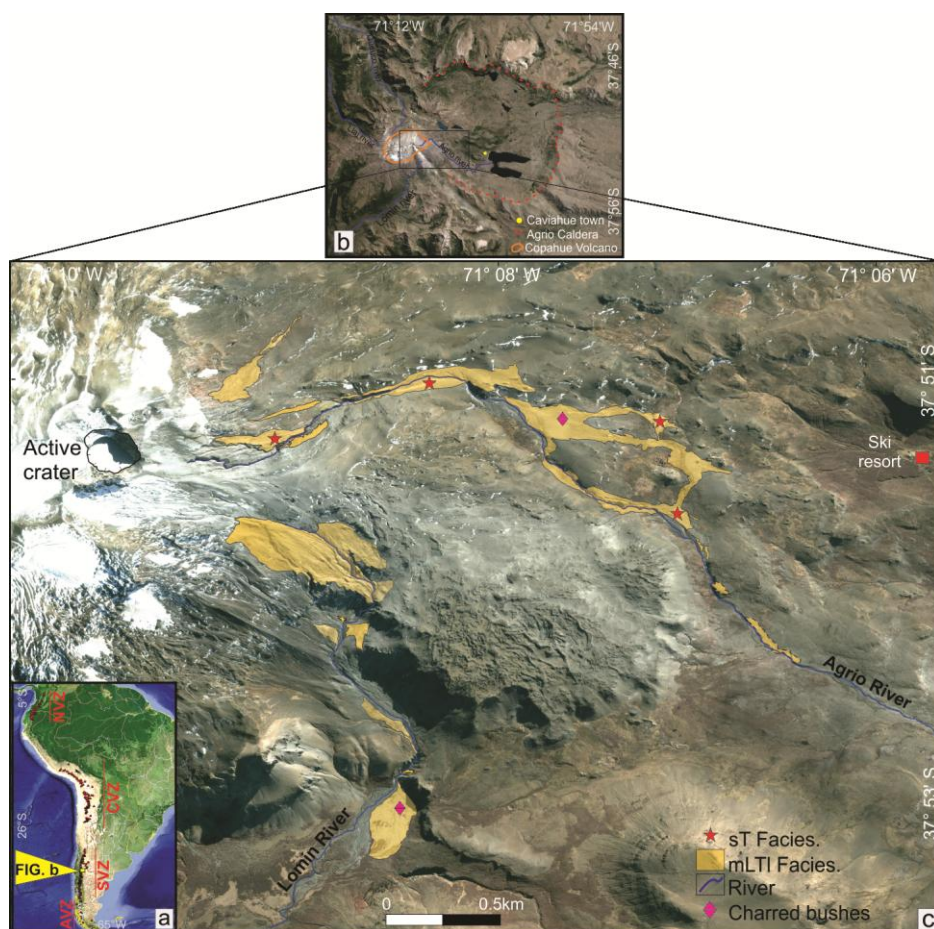


Figure 1



Figure 2



Figure 3

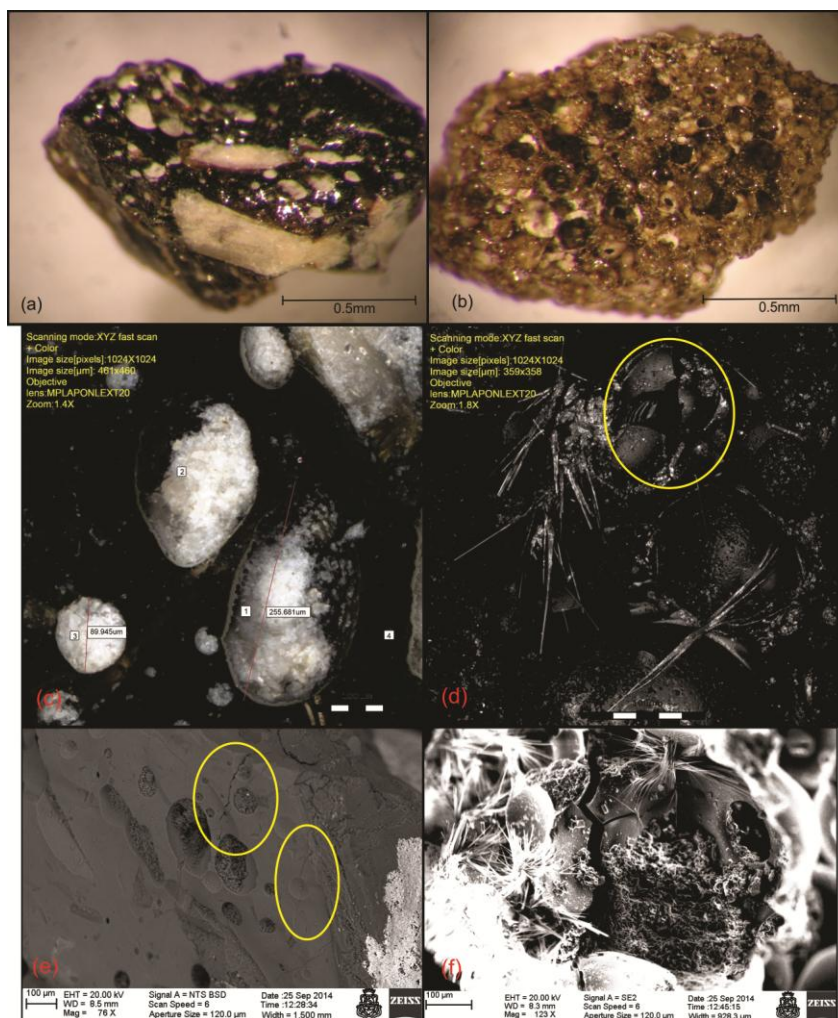


Figure 4

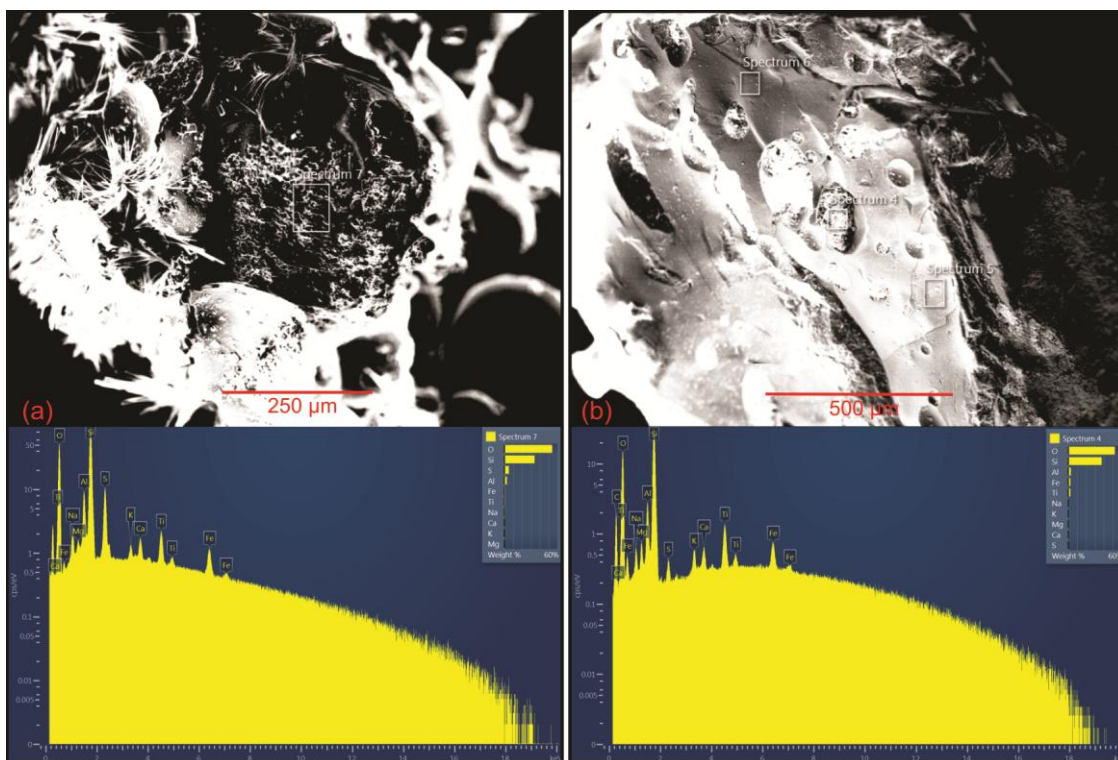


Figure 5

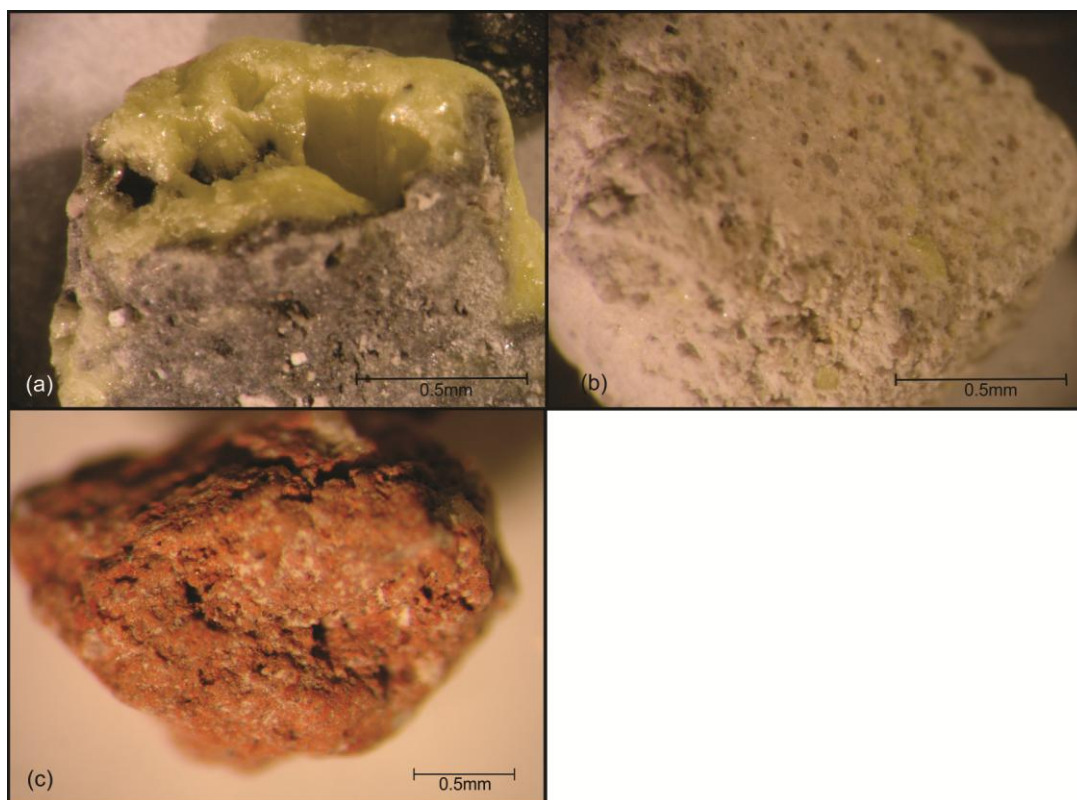


Figure 6

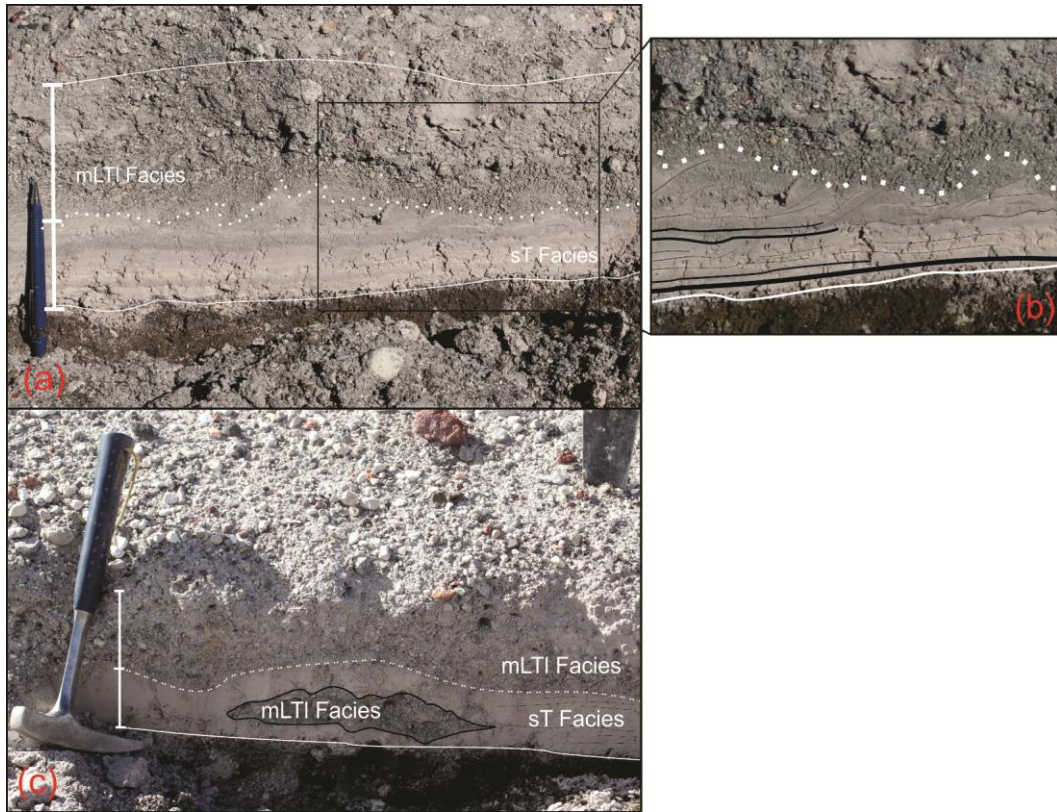


Figure 7

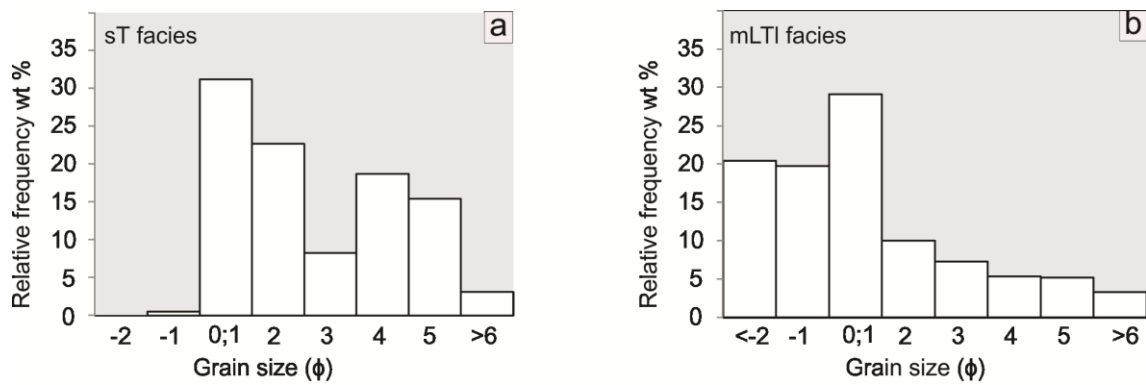


Figure 8

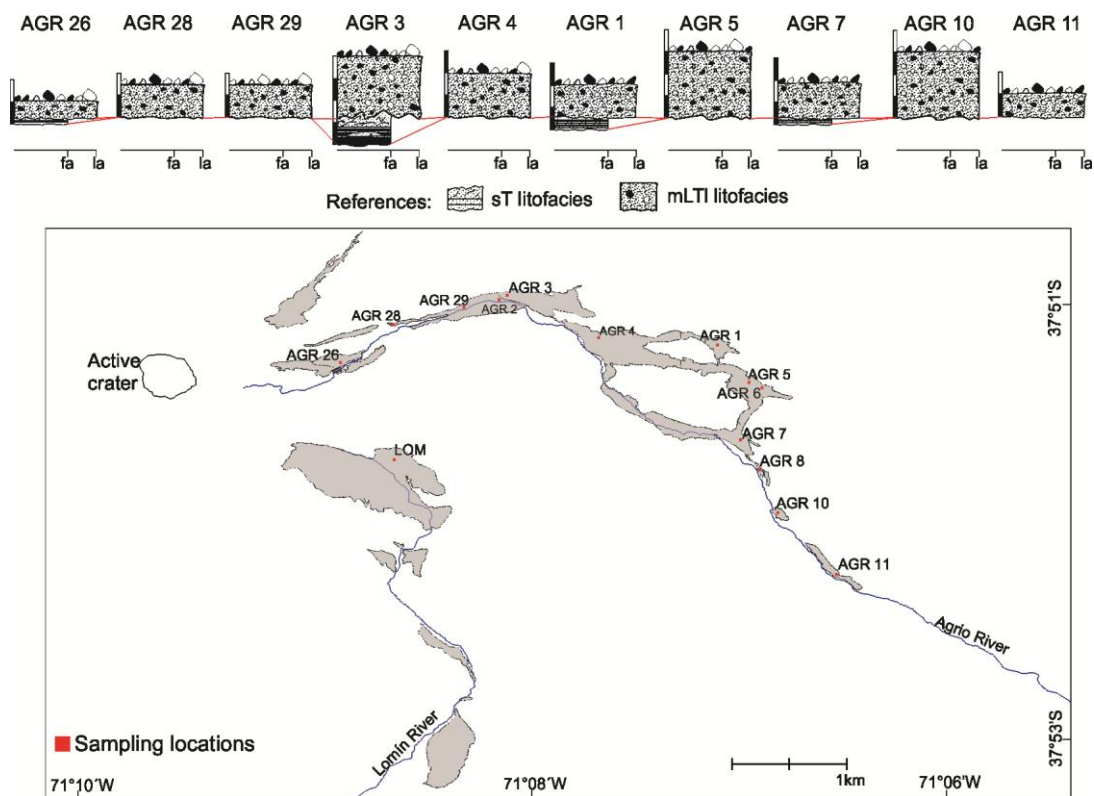


Figure 9



Figure 10

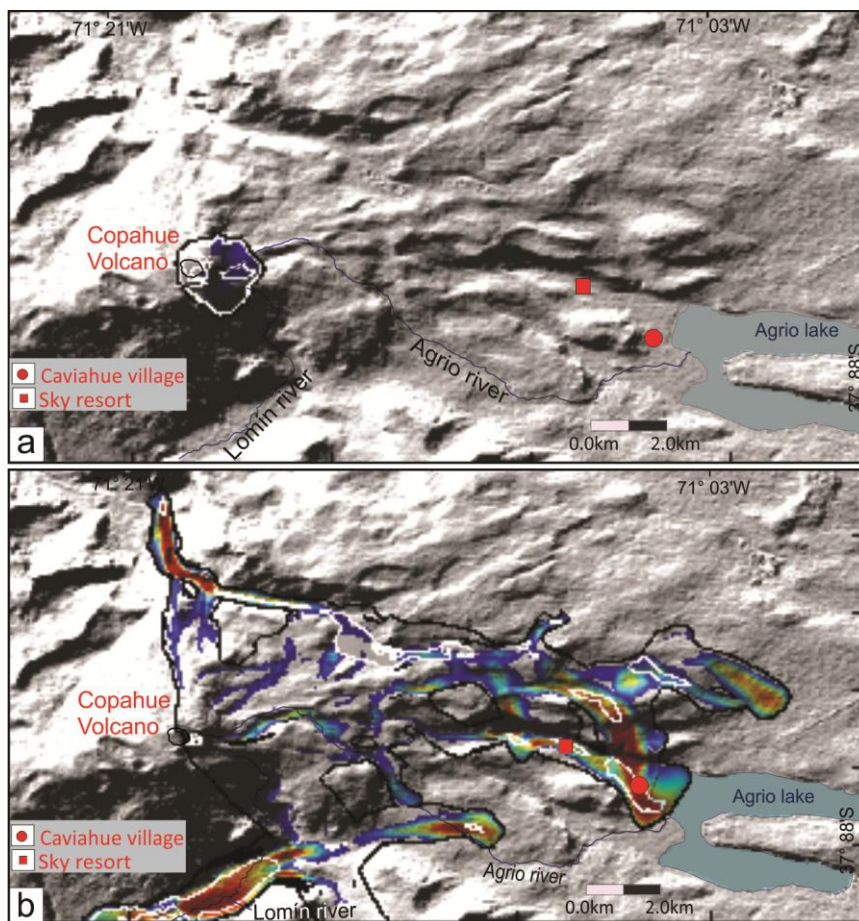


Figure 11

Highlights

- Phreatomagmatic eruption by interaction with hydrothermal system
- Pyroclastic density currents in Copahue volcano
- The facies architecture is a result of changes in the eruptive dynamic
- 2000 AD is the age proposed for this deposit

ACCEPTED MANUSCRIPT